TECHNICAL REPORT
66-46-CM

PHOTOGRAPHIC STUDY OF STRESS WAVE PROPAGATION AND CRACK GROWTH IN A TRANSPARENT PLASTIC

by

Anthony F. Wilde and John J. Ricca

Materials Research Branch

May 1966

UNITED STATES ARMY
NATICK LABORATORIES
Natick, Massachusetts 01760

Clothing and Organic Materials Division
C&OM-19

The findings in this report are not to be construed as an official Department of the Army position, unless so designated by other authorized documents.

Citation of trade names in this report does not constitute an official indorsement or approval of the use of such items.

DDC AVAILABILITY NOTICE

Distribution of this document is unlimited.

DISPOSITION INSTRUCTIONS

Destroy this report when no longer needed. Do not return it to the originator.

DISTRIBUTION OF THIS
DOCUMENT IS UNLIMITED

AD_____

TECHNICAL REPORT
66-46 CM

PHOTOGRAPHIC STUDY OF STRESS WAVE PROPAGATION AND CRACK GROWTH IN A TRANSPARENT PLASTIC

by

Anthony F. Wilde, Ph. D. John J. Ricca

Personnel Armor Materials Research Section
Clothing and Organic Materials Division

5 May 1966

Project Reference:
1L013001A91A

Series
C&OM-19

U. S. Army Materiel Command
U. S. ARMY NATICK LABORATORIES
Natick, Massachusetts

FOREWORD

The development of superior lightweight armor depends to a large extent upon better understanding of the various response processes which occur in the impacted materials. This requires an investigation into details of material behavior during and after a ballistic impact. Because of experimental difficulties, the development of tools and techniques for such studies has frequently been confined to situations involving less extreme conditions of mechanical loading. This report describes some of the early results of an investigation into two aspects of the response of a plastic to a low-speed mechanical impact.

Members of the Materials Research Branch of the Clothing and Organic Materials Division have conducted this study under Task 04 "Mechanical Properties of Organic Materials", of Project 1L013001A91A "In-House Laboratory Initiated Research and Development". The authors of this report wish to acknowledge the generous support given to the program by Dr. J. F. Oesterling and his Review Committee of the In-House Laboratory Independent Research Program.

GEORGE R. THOMAS, Ph.D.
Associate Director
Clothing & Organic Materials Division

APPROVED:

DALE H. SIELING, Ph.D.
Scientific Director

W. M. MANTZ
Colonel, QMC
Commanding

CONTENTS

CONTENTS (Continued)

LIST OF FIGURES

LIST OF TABLES

ABSTRACT

In order to develop techniques for studying the transient behavior of plastic materials subjected to mechanical impact, a preliminary photographic investigation was undertaken with an electronic image converter camera system. Two types of events were recorded with CR-39 plastic serving as the specimen material:

1. Stress pulses, produced in the plastic by mechanical impaction, were studied by observation of the resulting fringe patterns. The pulse fronts were characterized in terms of shape and propagation velocity. An empirical equation was derived to express the decrease in slope of segments of the pulse front as it propagated through the specimen.

2. Propagating cracks, generated in the plastic by mechanical impact, were subjected to photographic analysis. Crack propagation velocities and estimated crack initiation times were obtained. These served to yield a rough estimate of the magnitude of the incident longitudinal pulse level at which crack initiation occurred.

PHOTOGRAPHIC STUDY OF STRESS WAVE PROPAGATION AND CRACK GROWTH IN A TRANSPARENT PLASTIC

Introduction

In order to develop a better understanding of the behavior of plastic materials subjected to ballistic impact, members of this Laboratory have undertaken an investigation into some of the responses occurring during impaction of plastic specimens. It was desirable that this study include the magnitudes, durations, and time sequences of certain events preceding and accompanying failure of the specimen. For this study, two types of events were chosen; these were the incident stress pulse, and the beginning of crack growth. These events are important ones which must be included in any comprehensive investigation of ballistic impact and penetration.

Because stress wave propagation and crack growth occur rapidly, usually in times measured in microseconds, very fast detecting and recording techniques were required for study of these phenomena. In addition, it was necessary that the specimens be instrumented without unduly altering their behavior. Therefore photographic techniques were employed for observation of these dynamic material responses.

This report will describe in some detail the techniques and results of a preliminary investigation in which an electronic image converter camera was used to study stress wave propagation and crack growth generated in CR-39 plastic by low-speed mechanical impaction.

PART I. INSTRUMENTATION AND GENERAL PROCEDURE

In the course of developing suitable high speed photographic techniques for studying the birefringence accompanying the stress pulse in transparent plastics subjected to mechanical impact, it became evident that satisfactory data could not be obtained with a medium-speed camera (26,000 frames per second) whose first frame was taken at an uncontrolled time during a 38-microsecond time span(1). This 38-microsecond uncertainty represented, in some cases, an appreciable fraction of the time during which the first important events were in progress. In addition, the 38-microsecond period between each of the following frames was too great a time span for accurate delineation of the subsequent events. What was required was either a much higher-speed camera (to reduce the uncertainty of the time at which the first frame was taken and to reduce the time span between the following frames) or a camera whose individual exposures could be set independently at any desired times after generation of a synchronizing pulse. For this reason, a 4-unit electronic image converter camera was acquired. Each of the 4 pictures could be taken at independently preset delay times. This arrangement provided much greater flexibility for studying rapidly changing events.

1. Image converter camera

This image converter was an Abtronics, model 3-4R electronic camera, manufactured by Abtronics, Inc., Livermore, California.* This model contains four individual remote recording units, connected by cable to the control unit. Each recording unit produces one photograph. The major components of each recording unit are an image converter tube, a 135 millimeter, f/2.0 objective lens, and a Polaroid camera. The image converter tube serves as the shutter and is activated by a high voltage pulse. The duration of the exposure is determined by the pulse width and can be varied in steps from 5 nanoseconds to 1.0 microsecond. The delay time between each photograph can be varied from 0 to 10,000 microseconds. The image converter tube contains a cathode and an anode. An image of the object to be photographed is focused on the 2.5-inch diameter cathode. Application of the high voltage pulse accelerates photoelectrically emitted electrons from the cathode to the anode. A recreated image, formed on a phosphor layer, is photographed by the Polaroid camera.

2. Light source

The light source used to illuminate the photo field was a xenon flash lamp (General Electric FT-506) powered by a Beckman & Whitley model 357 flash unit. The flash unit had been modified to increase the intensity of the light pulse to a value estimated at approximately 10^7 peak beam candlepower. An oscilloscope record of the modified light pulse intensity appears in Figure 1. The total pulse duration was 4 milliseconds.

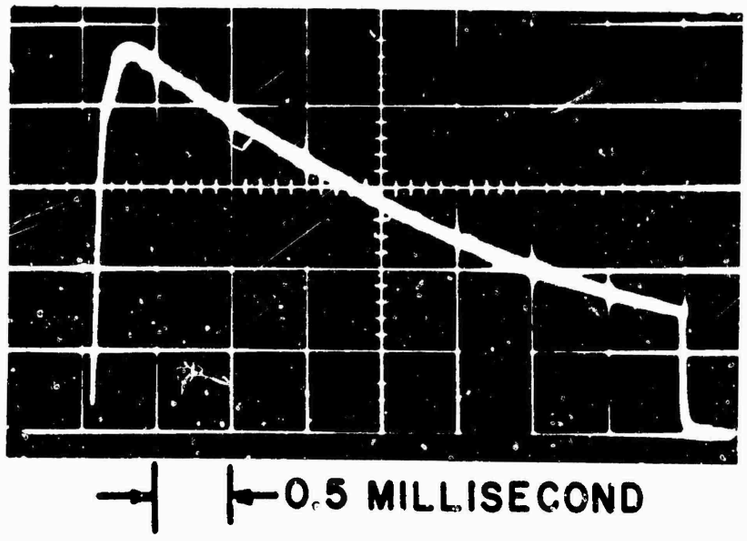

Figure 1 - Oscilloscope Record of the Modified Light Pulse Intensity

*This product line is now sold by Beckman & Whitley, Inc., San Carlos, California.

3. Polariscope, scale, chart, filters, film

To observe the birefringence produced in the impacted specimen, a dark-field circular polariscope was used. A scale and a resolution chart were also located in the photo field. To render these visible within the dark-field polariscope, one layer of transparent plastic tape was placed over them. This added retardation permitted enough light transmittance to silhouette the markings. Because a narrow bandwidth of light was required for good fringe resolution, two filters (Wratten 77A and 58B) were used; these were fastened to the front of each objective lens on the recording units. Polaroid film, type 47, speed 3000, was employed in each camera unit to record the images.

4. Small field

In spite of the high-speed Polaroid film, it was difficult to obtain good film exposures, owing to the great attenuation of light by the polariscope and the two filters. Hence, it was necessary to concentrate the light over a small field. This was done by placing the flash tube and its 4½-inch reflector about 2 inches from the first component of the polariscope. The field actually observed in the photographs was a circular one, about 3½ inches in diameter. Because of this small field size, it was not feasible to focus more than two of the four recording units to observe any one event. Hence, in all the results to be described, only two photographs were obtained for each event. For those events where four photographs are shown, the event had been repeated and two additional photographs were taken at different delay times. In some cases, this was repeated a third time to yield a series of six sequential photographs.

5. Specimen material: CR-39

Because it was required to observe birefringence in the impacted specimen, it was necessary that the specimen material be transparent and optically active (i.e., become birefringent when stressed). Previous work with CR-39 plastic in these Laboratories (1) had indicated that this material was suitable for such a study. CR-39 is a commercial polymer of allyl diglycol carbonate, available in sheets of various thickness. Strip specimens of this material, 1/4 inch thick and 1-1/4 to 1-1/2 inches wide, were used throughout the subject of this report. Static visual examinations of these specimens in the polariscope showed little or no optical nonuniformity both before and after nondestructive impact.

6. Arrangement of specimens, anvils, and impacting mechanism

For the stress wave study (Fig. 2, upper drawing), the CR-39 strip specimens were approximately 7-1/2 inches long. They were set in a 1/8-inch deep groove in a wood platform and butted against another plastic strip. Anvils were used both to prevent cracking of the specimen and to shape the pulse propagated into the specimen. The anvils were either blocks of CR-39, 1/4 inch thick, 1 inch high and 3/8 inch long, or blocks of lead,

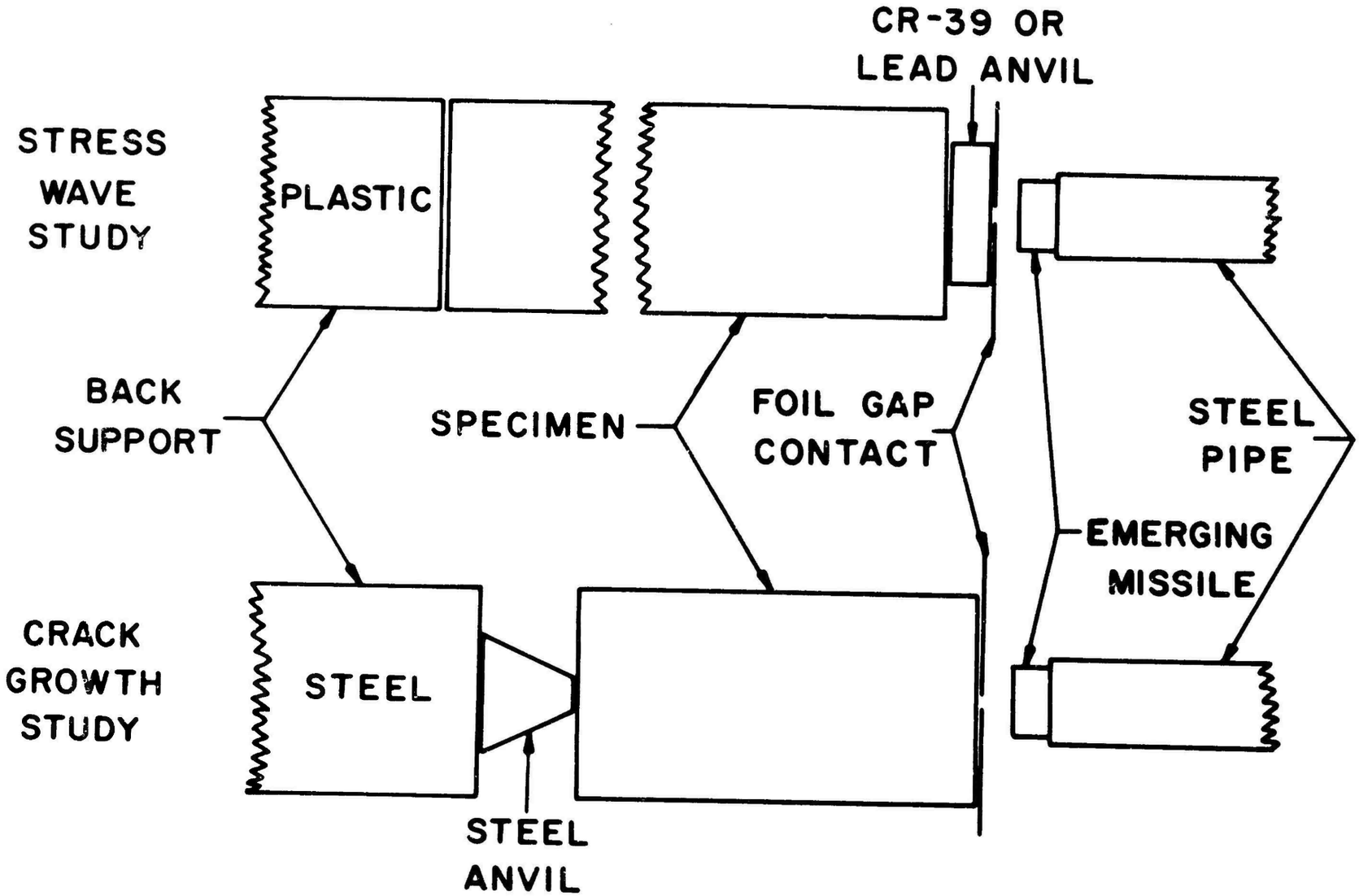

Figure 2 - Arrangement of Specimen, Anvil, Foil Gap Contact, and Impacting Apparatus

1/4 inch thick, 1 inch high, and 1/4 inch long. These were attached with Du Pont "Ducco" cement to the end of the specimen. Aluminum foil gap contacts were cemented to the other face of the anvils.

For the crack growth study (Fig. 2, lower drawing), the CR-39 specimens were 2-3/4 inches long. They also were mounted on the grooved platform. The steel anvil, cemented at the back edge of the specimen to generate cracks, was a trapezoid, 1/4 inch thick, 5/8 inch long, with front and rear edges 1/4 inch and 7/8 inch high, respectively. The back of the anvil butted against a steel strip. The foil gap contact was cemented directly to the front edge of the specimen.

The impacting mechanism has been described previously (1). Briefly, a right cylindrical steel missile (1 inch long and 1/2 inch in diameter) was propelled along a steel pipe (1/2 inch internal diameter) by the gas pressure applied from a helium gas cylinder. See Fig. 2. The end of the pipe was placed close enough to the end of the specimen so that the missile never completely emerged from the pipe. This was necessary to insure good impact alignment. When the end of the missile struck the thin aluminum foil gap contact, a synchronizing pulse was sent from a thyratron pulser to the image converter control unit. The values of time delay, programmed previously into the control unit, then determined the time at which each recording unit was activated. All photographic exposures were 1 microsecond in duration.

PART II. STRESS WAVE STUDY

A. Results and discussion: CR-39 anvil

1. Methods

When the steel missile impacted a CR-39 anvil (upper drawing of Fig. 2) at about 100 feet per second, a relatively steep pulse was produced in the attached CR-39 specimen. Three separate non-destructive impacts were made; two photographs were taken for each impact. The resulting six photographs, arranged in time sequence, are shown in Figure 3. The accompanying delay times refer to the elapsed time between impact on the front face of the anvil and the taking of the picture. Each exposure time was 1 microsecond. The upper strip in each photograph contains a scale marked in inches and a resolution chart for focusing purposes. For each photograph, measurements were made of the distance of each dark fringe from the end of the specimen facing the anvil and were converted to actual distances by comparison with the photographed scale. These measurements were made along the central axis of the specimen.

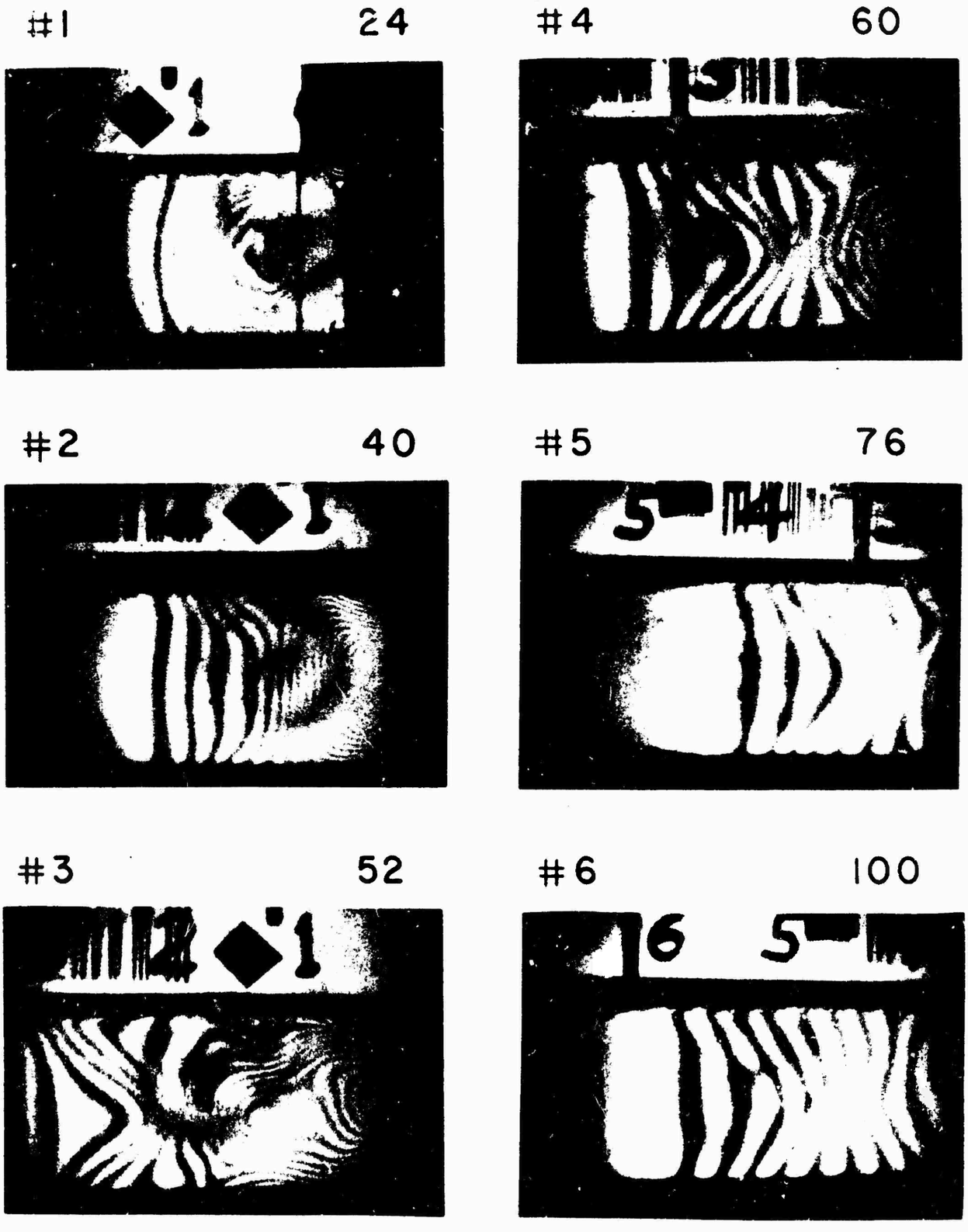

Figure 3 - Image Converter Photographs of Fringes Traveling in CR-39 Specimen After Impact Upon Attached CR-39 Anvil. (Delay times expressed in microseconds after impact. Exposure times of 1 microsecond.)

2. Description and significance of photographs

The first photograph shows the CR-39 anvil and the end of the CR-39 specimen. The fringes in the specimen are curved only slightly, showing that loading was fairly uniform over the end of the specimen. Here the first dark fringe has reached the 1-inch mark; the higher-order fringes lie progressively farther behind. The position and spacing of the fringes indicate both the distance traveled by the stress pulse and its general shape. The second photograph shows that the pulse front has progressed beyond the 2-inch mark. The third photograph shows a peculiar distortion in the fringe pattern, indicating nonuniform stress distribution in transverse sections of the specimen. This distortion is not evident in the first dark fringe; this fringe remains quite flat during its passage along the strip. Therefore the nonuniformity appears to be a function of the stress level. This transient distortion may also be partially due to some reflections of the pulse from the edges of the specimen during the early stages of propagation. The fourth and fifth photographs show continued progression of the pulse with gradual straightening of the distorted fringes. This growth and decay of distortion in the fringe pattern was repeatedly observed in other similar experiments. The sixth photograph shows that the pulse front has passed the 6-inch mark and that the fringe distortion has almost disappeared.

The fringe orders are plotted against their positions on the specimen in Figure 4. Each of the six curves refers to measurements made from the photograph taken at the specified delay time. Because the fringe order gives some measure of the stress or strain amplitude at that point, each curve represents, in effect, a profile of the pulse front at that particular time. One sees, therefore, a progression of the pulse front along the specimen axis, ranging up to a distance of about 5-1/2 inches. The transient distortion, noted previously, is seen most markedly in the third curve at 52 microseconds, and has virtually disappeared in the last curve at 100 microseconds. Because the usable light field was relatively small, the peak of the pulse is not seen in these photographs. Hence, the peak amplitude of the pulse is not known.

3. Slopes of pulse front smaller at longer delay times and apparent fringe velocity decreases with increasing fringe order

One sees in Figure 4 that the slopes of the curve are smaller at longer delay times. This indicated that the lower-order fringes appear to travel faster; the trend is shown graphically in Figure 5. Here the average apparent velocity of each fringe (measured between the 24- and the 100-microsecond positions to avoid the period of the distorted fringes) is plotted against the order of the fringe. There is a smooth decrease in fringe velocity with increasing fringe order. This trend has been observed by others (2), and is caused by dispersion effects which change the shape of the pulse as it propagates along the specimen. Because this material is viscoelastic in nature, some of the dispersion noted here is produced by the effects of attenuation. In general, attenuation effects vary with the mechanical properties of the material (3).

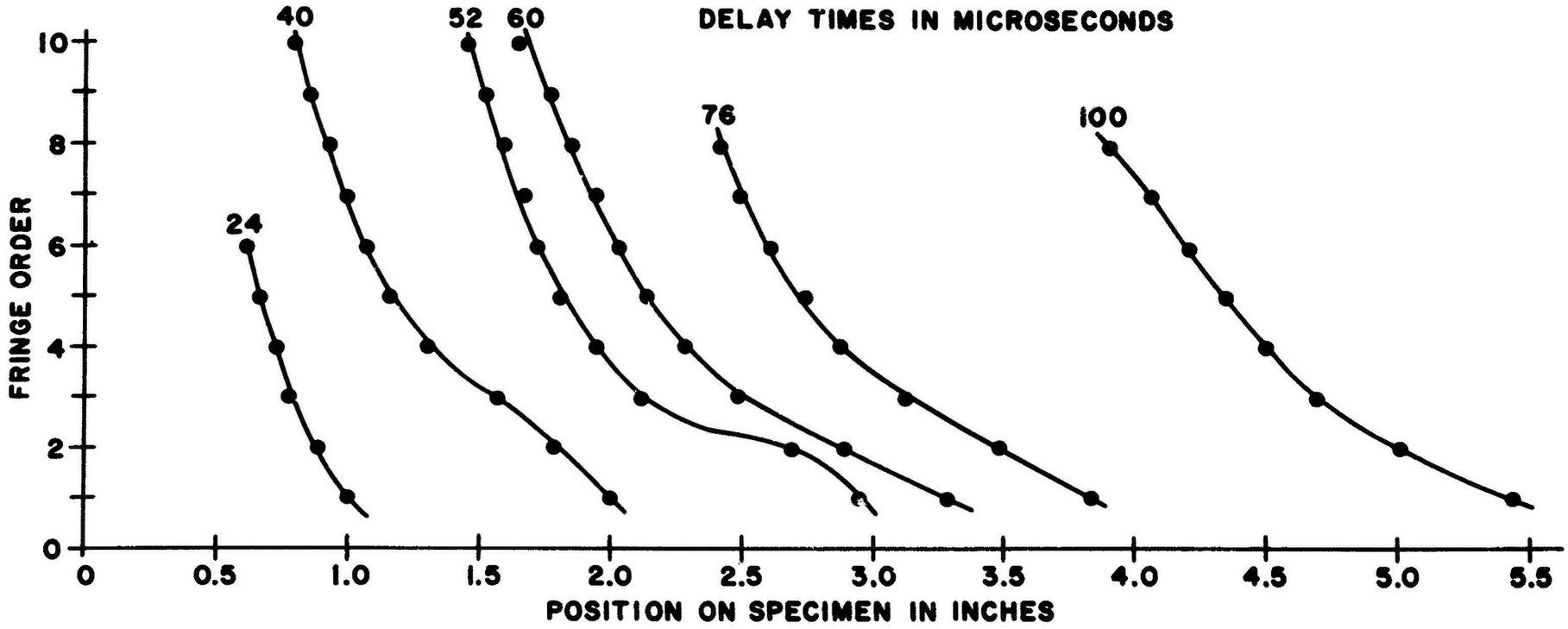

Figure 4 - Fringe Order Plotted Against Position Along the Specimen Axis at Each Delay Time. (Delay times expressed in microseconds after impact)

4. Average longitudinal strain gradient between fringes decreases monotonically with increasing distance

The slope of the pulse front was characterized by considering small segments of each of the curves in Figure 4. For example, consider fringe orders 5 and 6. These high-order fringes were chosen to avoid the transient distortion in the lower-order fringes. From previous wave studies of birefringence and strain in impacted CR-39 specimens, conducted in these Laboratories (1), the approximate dynamic longitudinal strain-fringe constant for CR-39 had been determined. The value was 255 microstrain-inch thickness per fringe. This value was used along with the positions of fringe orders 5 and 6 in Figure 4 to determine the average longitudinal strain gradient between fringe orders 5 and 6. This gradient is plotted in Figure 6 as a function of the distance traveled by fringe order 5. The strain gradient decreases monotonically with increasing distance. This again shows the effects of attenuation and dispersion in the specimen.

5. Equation to express decrease of longitudinal strain gradient with increase in distance traveled by this portion of pulse

In order to characterize more quantitatively this decrease of the pulse slope or strain gradient with distance, attempts were made to fit these results to an empirical equation. The data in Figure 6 are shown in a log-log plot in Figure 7. Although there is still some scatter, a straight line derived by the method of least squares represents the trend to a fair degree. The measured slope was -0.6. This then yields the equation

$$g = C_1 d^{-0.6} \qquad (1)$$

where g is the longitudinal strain gradient in percent strain per inch
d is the distance traveled in inches, and
C_1 is a constant

This equation represents, in an empirical fashion, the decrease of pulse slope with increase in the distance traveled by this portion of the pulse. The negative exponent is a measure of this change. A similar value for this exponent was obtained by treating fringe orders 7 and 8 and fringe orders 1 and 2 (excluding the distorted region) in the same fashion.

B. Results and discussion: Lead anvil

1. Methods

Another series of impacts at about 100 feet per second was conducted, in which a lead anvil was used (upper drawing of Fig. 2). The resultant stress pulse in the attached CR-39 specimen was much less steep at its leading edge than in the experiments where the CR-39 anvil was used. Two separate non-destructive impacts were made and two photographs were taken for each impact.

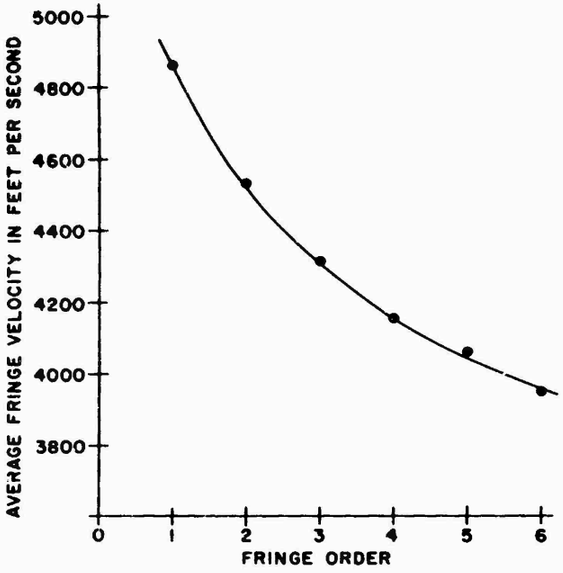

Figure 5 - Average Fringe Velocity Plotted Against Fringe Order

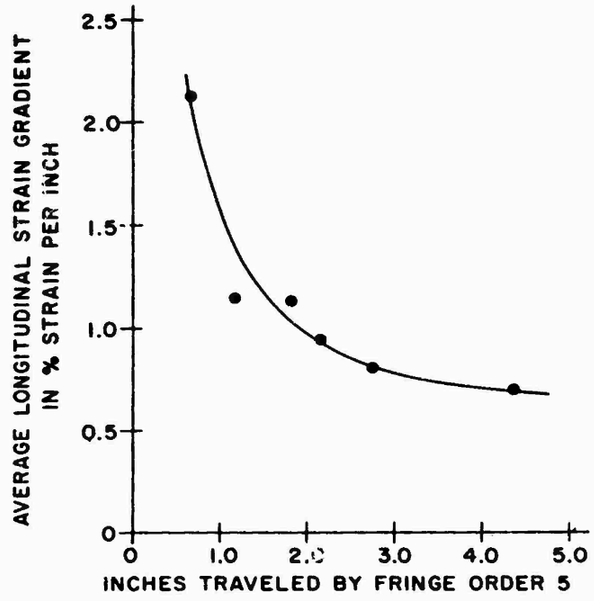

Figure 6 - Average Longitudinal Strain Gradient Between Fringe Orders 5 and 6 Plotted Against Distance Traveled by Fringe Order 5.

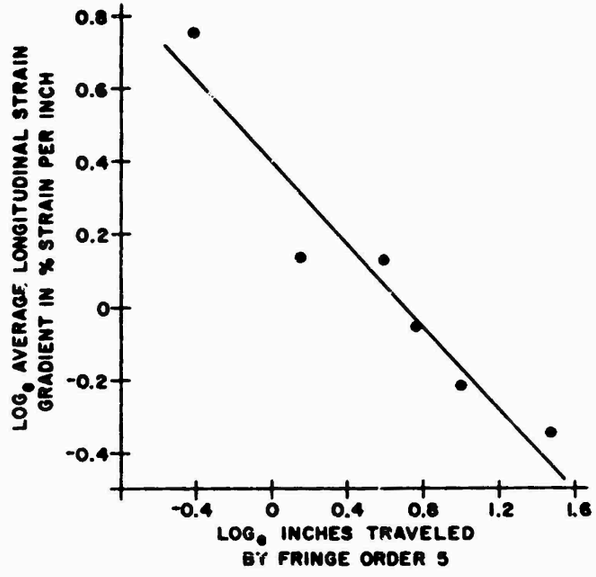

Figure 7 - Natural Logarithm Average Longitudinal Strain Gradient Between Fringe Orders 5 and 6 Plotted Against Natural Logarithm Distance Traveled by Fringe Order 5.

The resulting four photographs, arranged in delay time sequence, appear in Figure 8. Each exposure was 1 microsecond in duration. As before, the distance of each dark fringe from the impacted end of the specimen was measured along the central axis of the specimen.

2. Description of photographs

The first photograph shows a nearly concentric set of fringes appearing to emanate from the middle of the impacted edge of the specimen. This indicates that the pulse was propagating in two dimensions, both longitudinally and laterally. Apparently the 1/4-inch lead anvil transmitted the load mainly to the central area of the edge of the specimen. This produced more of a point loading of the specimen than in the previous example where the 3/8 inch CR-39 anvil produced a more uniform loading over the entire edge of the specimen. The second photograph shows that the leading fringes have reached the specimen edges and are not very curved, whereas the following higher-order fringes are still highly curved. This one photograph, therefore, shows the transition from 2-dimensional propagation, both longitudinal and lateral, to an approximately 1-dimensional longitudinal propagation. The third and fourth photographs show the progress of the leading fringes as they approach the 6-inch mark.

It is apparent that the fringe spacing at 100 microseconds in Figure 8 is much greater than that at 100 microseconds in Figure 3. This difference in fringe spacing between the two specimens is some measure of the difference in steepness of the pulse front, and is a consequence of the different loading conditions experienced by the specimens. This difference in specimen loading is probably due both to greater pulse degradation in the lead anvil than in the CR-39 anvil and to the geometrical expansion occuring in the lead-loaded specimen between the point of loading and the full specimen width.

A plot of the fringe orders versus their positions on the specimen appears in Figure 9. Each of the four curves is constructed from measurements made from the photograph taken at the specified delay time. Again, each curve represents, to a certain extent, a profile of the leading edge of the pulse at that particular time. There is no evidence of the transient distortion noted in the previous series. As before, the peak of the pulse was not visible because of the small light field. The vertical broken line is an approximate indication of the transition from 2- to 1-dimensional propagation as seen in the second photograph of Figure 8.

3. Change in slope of pulse front with increasing distance

Figure 9 shows the marked change in slope of the pulse front with increasing distance. The resultant effect on the apparent fringe velocities is similar to that shown in Figure 5; the fringe velocity decreases monotonically with increasing fringe order.

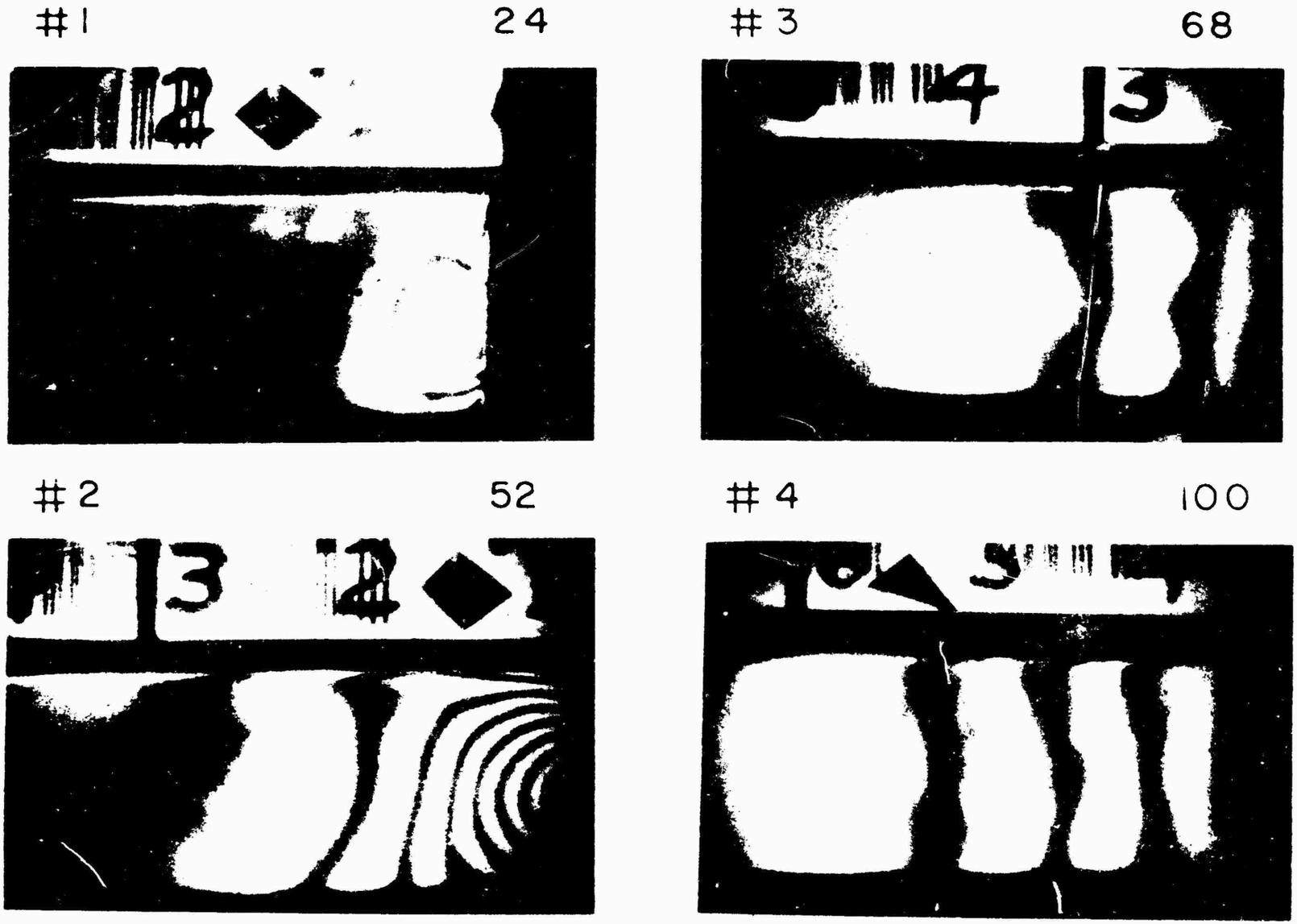

Figure 8 - Image Converter Photographs of Fringes Traveling in CR-39 Specimen After Impact Upon Attached Lead Anvil. (Delay times expressed in microseconds after impact. Exposure times of 1 microsecond.)

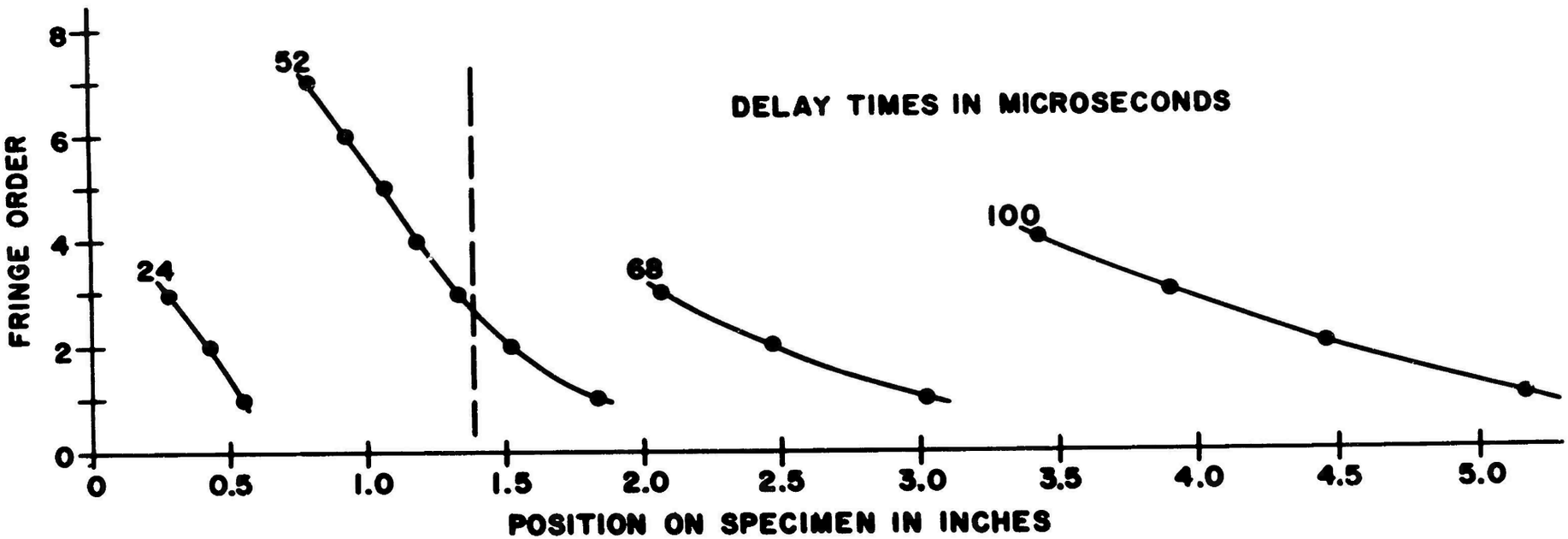

Figure 9 - Fringe Order Plotted Against Position Along the Specimen Axis at Each Delay Time. (Delay times expressed in microseconds after impact.)

4. Average longitudinal strain gradient between fringes decreases monotonically with increasing distance

The slope of a segment of the pulse front was characterized by examining fringe orders 1 and 2 in Figure 9, (excluding the 24-microsecond data to eliminate the 2-dimensional region). Use was made of the longitudinal strain-fringe constant to convert the fringe orders and fringe distances to the average longitudinal strain gradient between fringe orders 1 and 2. This gradient appears in Figure 10 as a function of the distance traveled by fringe order 1. As with the CR-39 anvil, the average longitudinal strain gradient decreases monotonically with increasing distance, owing to the effects of attenuation and dispersion in the specimen.

5. Equation to express decrease of longitudinal strain gradient with increase in distance traveled by this portion of pulse

A log-log plot of the data in Figure 10 is shown in Figure 11. A straight line drawn through these points by the method of least squares has a slope of -0.8, yielding the empirical equation

$$g = C_2 d^{-0.8} \qquad (2)$$

where g is the longitudinal strain gradient in percent strain per inch
d is the distance traveled in inches, and
C_2 is a constant

C. General discussion

It is interesting to note that the value of the negative exponent in Eq.(2) is somewhat close to that in Eq.(1), considering the approximate nature of the measurements which could be made from the photographs. Agreement of this sort tended to confirm the suitability of the foregoing empirical treatment in describing the behavior of the pulse front, especially considering that the measurements in the two cases were made with differently shaped pulses and at different strain levels during the leading edge of the pulse. This suggests that this exponent may be a useful measure of the overall dispersion processes, some of which occur in the plastic specimen as a result of various molecular motions which cause energy dissipation and pulse attenuation.

It is realized that the fringe pattern or longitudinal strain front seen here cannot be directly subjected to a viscoelastic analysis. Instead, one could resolve the pulse into a series of Fourier components and treat the behavior of each one in accordance with viscoelasticity principles(3). In this report our observation and treatment has been concerned only with the total pulse, not with the behavior of these components. It is not claimed that Eqs(1) and (2) are the only types of empirical expressions which would describe the data. Certainly, more rigorous curve-fitting treatments might express the data better. However, the above equations are simple and reasonably satisfactory. The applicability of these equations is claimed only for CR-39 specimens of this size and only for pulses of this general shape and magnitude.

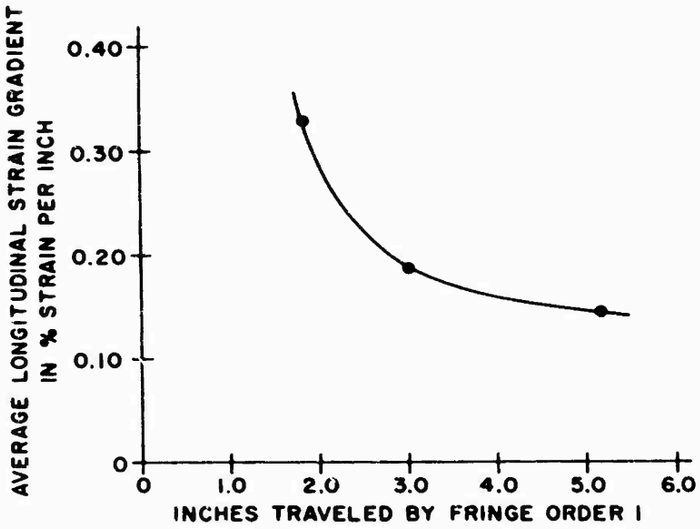

Figure 10 - Average Longitudinal Strain Gradient Between Fringe Orders 1 and 2 Plotted Against Distance Traveled by Fringe Order 1.

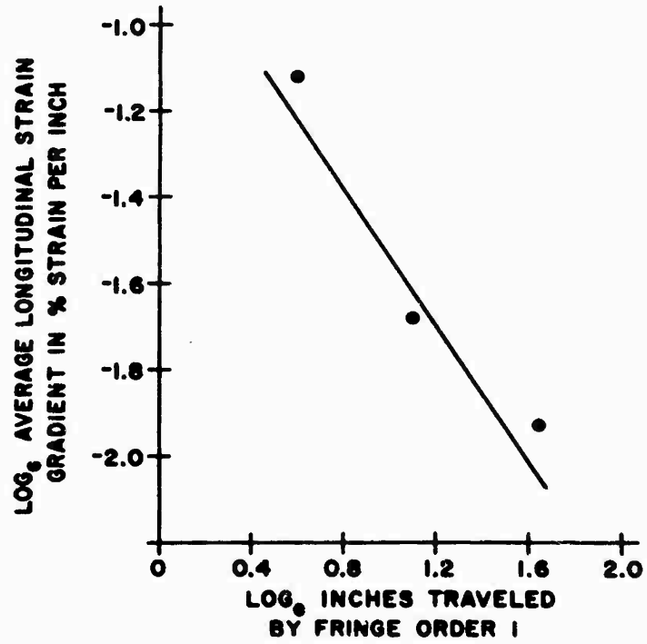

Figure 11 - Natural Logarithm Average Longitudinal Strain Gradient Between Fringe Orders 1 and 2 Plotted Against Natural Logarithm Distance Traveled by Fringe Order 1.

PART III. CRACK GROWTH STUDY

1. Methods

Impaction at about 100 feet per second of the CR-39 specimen, as shown in the lower drawing of Figure 2, produced both a fringe pattern and growing cracks. These are visible in the Polaroid photographs shown in Figure 12. Two pictures were taken for each impact,(E-31 and E-37), 135 and 170 microseconds after impaction. The scale at the top of each photograph is marked at 1/2-inch intervals. Impact occurred at the right end of the specimen. Because the trapezoid-shaped anvil produced large shear stresses at the back end of the specimen, the cracks began at the left end, as seen in the photographs, and grew toward the right. No cracks were generated at the impacted edge of the specimen; possibly there was some reinforcement by the contact foil cemented to this edge of the specimen.

2. Photographs: fringe patterns

The fringe patterns are interesting because of their unusual shapes in the vicinity of the cracks. The patterns appear as cusps which point to the heads of the growing cracks. These cusps indicate unusual stress distributions and are presumably related to the crack growth process.

3. Average crack velocities calculated

From measurements made of the crack head positions at each of the two delay times it was possible to calculate an average crack velocity. These are given in Table I.

TABLE I: CRACK VELOCITY AND CRACK INITIATION TIME

Experiment	Crack Location	Average Crack Velocity	Estimated Crack Initiation Time
		ft/sec	μsec
E-31	Top	1660	40
	Middle	1370	31
E-37	Top	1590	43
	Middle	1680	49
	Bottom	1610	49

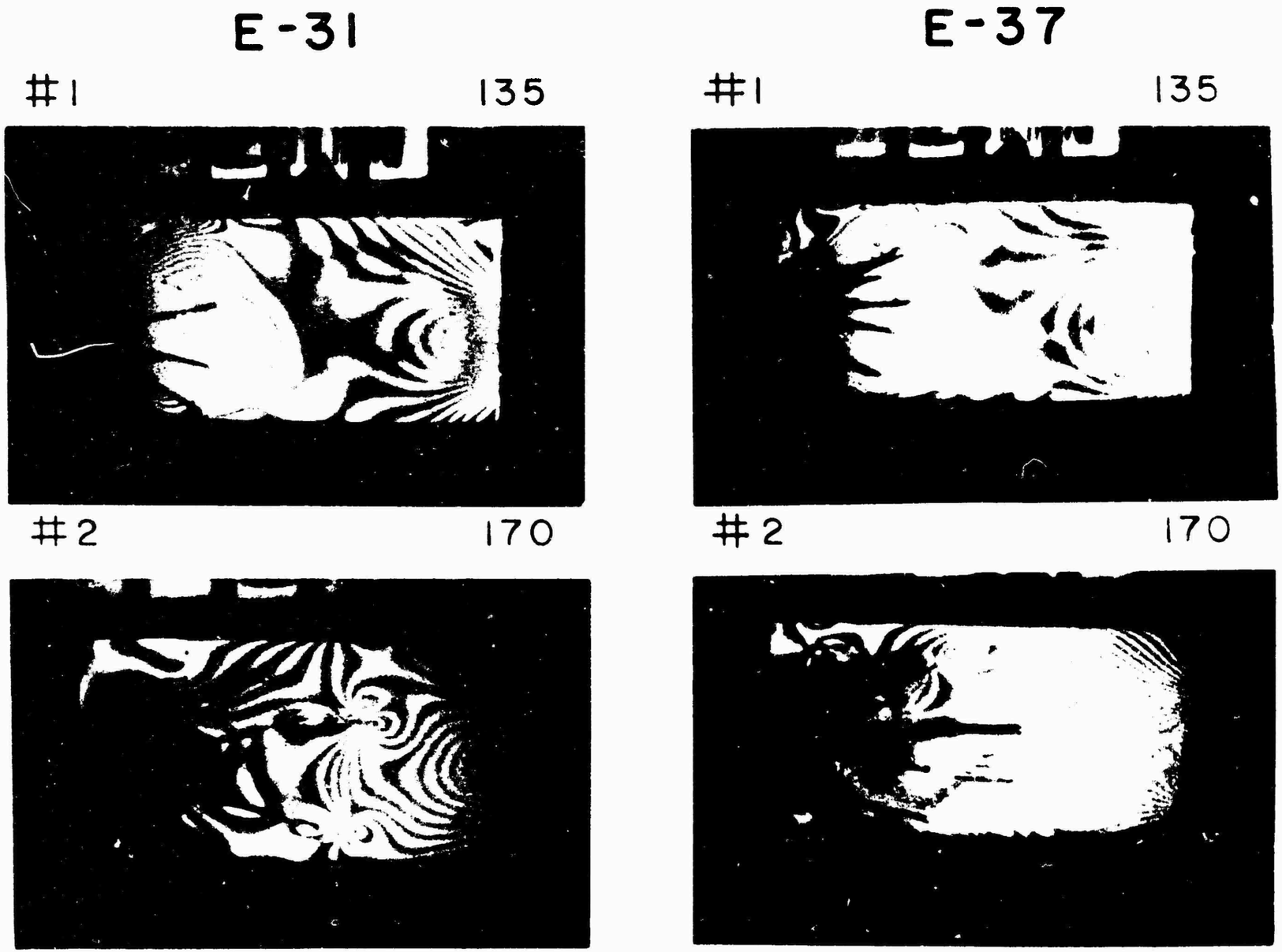

Figure 12 - Image Converter Photographs of Cracks Growing in CR-39 Specimen From the Left End After Impact at the Right End. (Delay times expressed in microseconds after impact. Exposure times of 1 microsecond.)

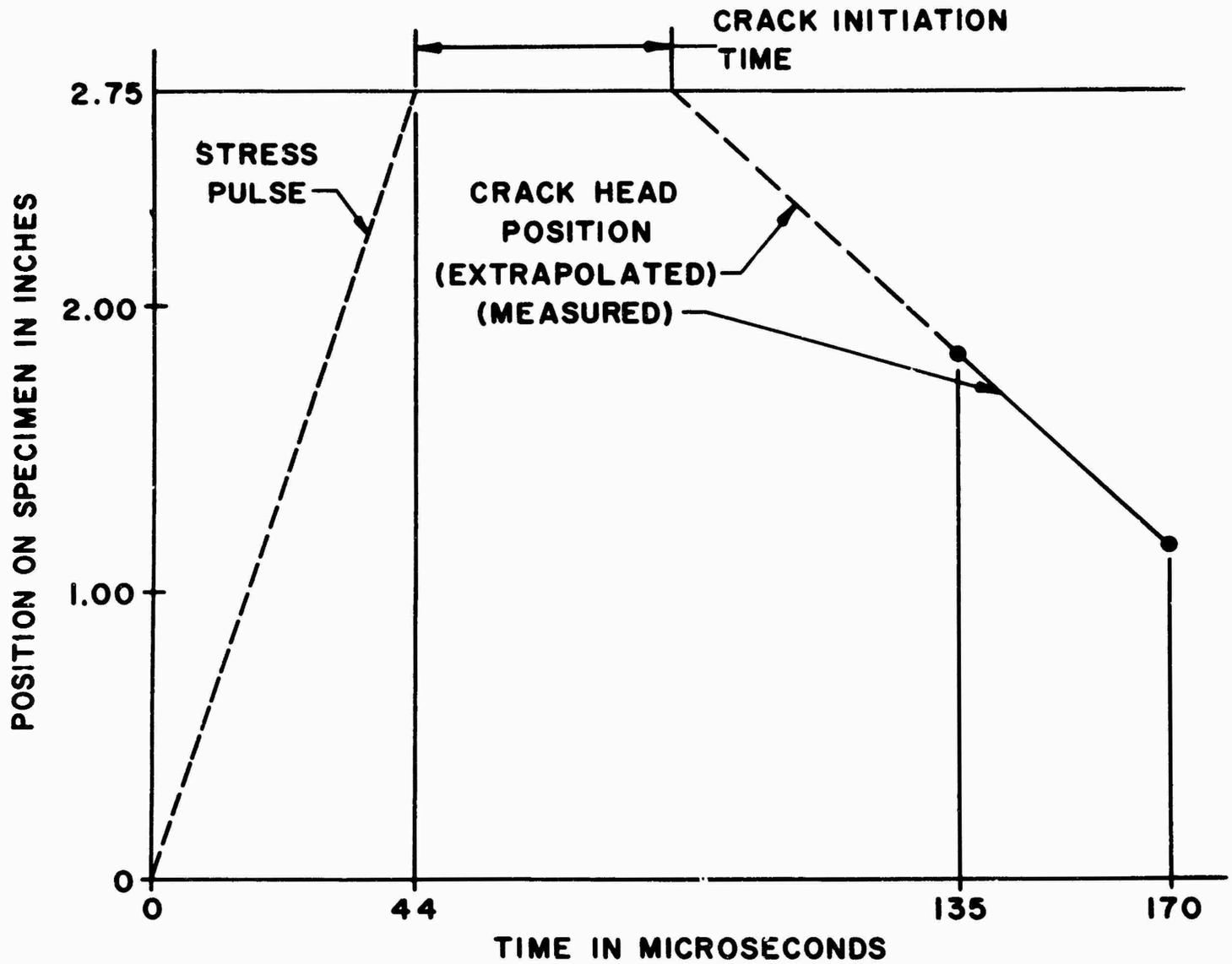

Figure 13 - Schematic Diagram of Position on the Specimen of Stress Pulse and Crack Head as Functions of Time After Impact. (Crack initiation time obtained from the double extrapolation.)

It is seen that the average crack velocities are quite close in value except for one which is somewhat lower. These velocities fall in the same general range as those reported for Plexiglas by Schardin (4). Very little information is available concerning crack propagation velocities in plastic materials; however, it has been stated (4) that although different crack velocities occur in plastic materials, each one, once it has appeared, is nearly stable.

4. Crack initiation time estimated

It is interesting to study the crack growth in some detail, especially to estimate the time at which crack initiation occurred. It was assumed that each crack propagated at a constant velocity; the crack growth was then extrapolated backward in time to the back edge of the specimen where initiation presumably had occurred. It is believed that the gross breakup of the specimen in the vicinity of the anvil did not occur until after passage of the growing cracks through this region. Use of the average value of stress pulse velocity in CR-39 (1)(16 microseconds per inch) permitted the determination of the time after impact at which the leading point of the preceding stress pulse had reached the back end of the specimen. These two extrapolations yielded the elapsed time between the arrival of the incident stress pulse and the initiation of the crack. These time relationships are shown schematically in Figure 13. The position on the specimen of the incident stress pulse and of the crack head are given as functions of time after impact. The elapsed time difference at the back edge of the specimen was designated as the crack initiation time and is given in Table I.

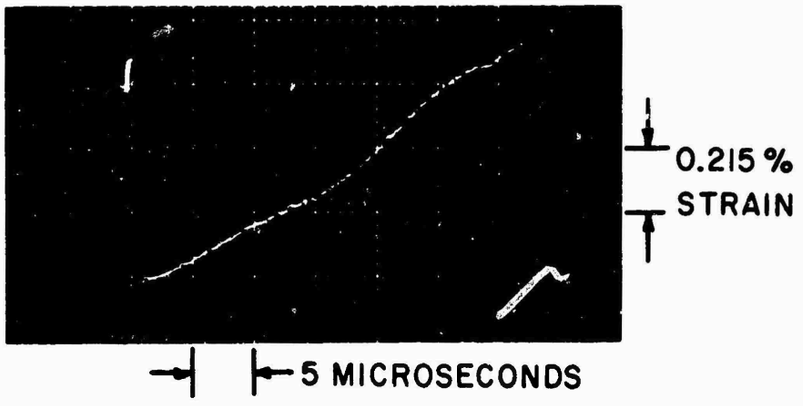

Figure 14 - Oscilloscope Record of the Leading Edge of a Longitudinal Strain Pulse in CR-39 at the Gage Site (6-3/4 inch from impacted end of anvil) as a Function of Time

5. Magnitude of incident longitudinal pulse estimated at time of crack initiation

Use of this crack initiation time then permitted a rough estimate of the magnitude of the incident longitudinal pulse at the back end of the specimen at the time of crack initiation. This was done by using unpublished strain gage data obtained during similar impacts on CR-39 strip specimens (1). The result produced with a 3/8-inch CR-39 anvil cemented to a CR-39 specimen in this previous work is shown in the strain gage record of Figure 14.

This gives the longitudinal strain as a function of time at the strain gage site, located 6-3/8 inches from the impacted end of the anvil. To estimate the shape of the strain pulse at a distance of 2-3/4 inches from the impacted end (to correspond to the position where crack initiation had occurred in the present experiments), use was made of Eqs (1) and (2) to estimate an average exponent value of -0.7, to give the equation

$$g = C_3 d^{-0.7} \qquad (3)$$

in the same units as the previous equations. At a distance of 6-3/8 inches from the impacted end, the average rate of the main portion of the leading edge of the pulse in Figure 14 is 28,000% strain per second. This is roughly equivalent to a gradient of 0.45% strain per inch, calculated from the average pulse velocity. A log-log plot of Eq. (3) was used to estimate a leading-edge gradient of 0.80% strain per inch at a distance of 2-3/4 inches from the impacted end. This was converted back to a rate of 50,000% strain per second at the 2-3/4 inch distance.

The average crack initiation time for the two experiments listed in Table I was 35 and 47 microseconds, respectively. A time of 5 microseconds was subtracted from each of these to yield the approximate length of time during which the strain increased at a significant rate. (The first 5 microseconds of the longitudinal strain pulse, such as that of Figure 14, has produced relatively little increase from the zero or base-line value.) Applying these adjusted values of 30 and 42 microsecond rise times to the leading edge of the new pulse derived from that of Figure 14 gives strain magnitudes of about 1.5 and 2.1 percent, respectively. This would then give the longitudinal strain at the back edge of the specimen at the time of crack initiation, if one neglects the presence of the interfaces at the back edge of the specimen.

6. Pulse reflections at back edge of specimen: role in creating unequal stress levels and causing cracks

Consideration was then given to the pulse reflections at the back edge of the specimen. It is evident from the lower drawing of Fig. 2 that two types of interfaces were present: specimen-air, and specimen-steel. In the region of the former interface, the pulse reflected back into the CR-39 specimen would be tensile, thus giving zero stress at the back surface of the specimen. In the region of the latter interface, the reflected pulse would be compressive and would thus add to the remainder of the incident pulse. The assumption was made that this rapidly-rising incident pulse was elastic in nature. Then the magnitude of the reflected pulse, σ_R, can be related to the incident pulse magnitude, σ_I, by the following expression:

$$\frac{\sigma_R}{\sigma_I} = \frac{Z_s - Z_p}{Z_s + Z_p} \qquad (4)$$

where Z_s and Z_p are the acoustic impedances of steel and CR-39, respectively.

This ratio of reflected to incident pulse magnitude is about 91%. Thus the total stress level in the specimen, at the interface backed up by steel, was about 1.91 times the incident stress.

Table II gives a summary of these results together with published values of the static compressive and tensile strengths of CR-39.

TABLE II: ESTIMATED PULSE LEVELS AT TIME OF CRACK INITIATION. COMPARISON WITH COMPRESSIVE AND TENSILE STRENGTHS OF CR-39

Estimated incident longitudinal compressive strain at time of crack initiation	1.5 - 2.1 percent
Estimated incident longitudinal compressive stress at time of crack initiation	7100-9900 psi[a]
Total estimated stress level at steel-backed interface at time of crack initiation	13,500-18,900 psi[b]
Static strength of CR-39	
Compressive	23,000 psi[c]
Tensile	5,800 psi[c]

[a] Computed from the estimated longitudinal strain together with the value of 4.7×10^5 psi for the dynamic modulus(1)

[b] Computed with the factor of 1.91 obtained from Eq(4)

[c] Obtained from PPG Chemicals Bulletin No. 307 (5)

It is seen that the total compressive stress level at the steel-backed interface (at the time of crack initiation) is less than the static compressive strength of the material. This inequality would probably be even larger if one considered the dynamic compressive strength of the material, since the dynamic value is presumably somewhat larger than the given static value. Therefore at the steel-backed edge of the specimen, compressive failure would not occur. Neither would it occur at the air-backed edge of the specimen where the stresses would be zero. Hence, it seems most likely that failure began at the boundary between these two regions where the specimen would undergo a shearing effect. The corners of the anvil represented points in the back edge of the specimen across which there was a large shearing effect due to these unequal stress levels (0 and 13,500 to 18,900 psi). This caused generation of the cracks. Although the actual stress and strain levels near the back edge were not measured directly (these stress and strain distributions would be complex because of the discontinuous boundary conditions), the foregoing estimation of the magnitude of the longitudinal stress and strain is a measure of the incident pulse level at which the shearing effect caused the crack initiation.

Even though this has been a very much simplified and approximate analysis, it does give some quantitative estimate of the pulse magnitude required to generate cracks in CR-39 plastic when this material is subjected to the pulses and geometrical constraints described above. Data of this sort, when obtained for a variety of plastics, may be very useful in explaining observed differences in cracking and spalling behavior of specimens subjected to ballistic impact.

Summary and conclusions

In the absence of peak values of the strain pulse and without resolution of the pulse into its Fourier components, empirical data can be obtained which describe certain propagation and dispersion effects occurring in impacted transparent plastic specimens. In addition, it appears possible to measure crack velocities and to estimate values of pulse levels at which cracks are initiated under certain conditions of loading.

It is concluded that high-speed photographic studies of this nature will be capable of yielding much useful information about the transient responses of transparent materials subjected to impact loading. These techniques should prove useful in more extended and more detailed studies of materials undergoing actual ballistic impact.

References

1. Wilde, A.F., J. J. Ricca, and F. deS. Lynch, Study of Dynamic Birefringence and Strain Produced in Transparent Polymers by Mechanical Impact, Tech. Report 66-6CM, Clothing and Organic Materials Division, U.S. Army Natick Laboratories (1966).

2. Dally, J. W., W. F. Riley, and A. J. Durelli, A Photoelastic Approach to Transient Stress Problems Employing Low-Modulus Materials, J. Appl Mechanics, 26, 613(1959).

3. Kolsky, H., Stress Waves in Solids, Republished by Dover Publications, Inc.(1963); Kolsky, H., The Propagation of Stress Pulses in Viscoelastic Solids, Phil Mag, 8th Series, 1, 693(1956).

4. Schardin, H., Velocity Effects in Fracture, a paper in "Fracture" (Proc of Intl Conf). Ed. by B.L. Averbach et al. The M.I.T. Press, Cambridge, Mass., p. 297 (1959).

5. Pittsburgh Plate Glass Co., Chemical Division, Market Development Bulletin No. 307 (Revised Apr. 11, 1962).

Unclassified
Security Classification

DOCUMENT CONTROL DATA - R&D
(Security classification of title, body of abstract and indexing annotation must be entered when the overall report is classified)

1. ORIGINATING ACTIVITY (Corporate author) U.S.Army Natick Laboratories Natick Massachusetts 01760	2a. REPORT SECURITY CLASSIFICATION Unclassified 2b GROUP

3. REPORT TITLE

PHOTOGRAPHIC STUDY OF STRESS WAVE PROPAGATION AND CRACK GROWTH IN A TRANSPARENT PLASTIC

4. DESCRIPTIVE NOTES (Type of report and inclusive dates)

Interim Progress Report November 1964 to August 1965

5. AUTHOR(S) (Last name, first name, initial)

Wilde, Anthony F. and Ricca, John J.

6. REPORT DATE	7a. TOTAL NO. OF PAGES	7b. NO. OF REFS
May 1966	23	5

8a. CONTRACT OR GRANT NO.	9a. ORIGINATOR'S REPORT NUMBER(S) 66-46-CM
b. PROJECT NO. 1L013001A91A	
c.	9b. OTHER REPORT NO(S) (Any other numbers that may be assigned this report) C&OM-19
d.	

10. AVAILABILITY/LIMITATION NOTICES

Distribution of this document is unlimited.
Release to CFSTI is authorized.

11. SUPPLEMENTARY NOTES	12. SPONSORING MILITARY ACTIVITY
	U.S.Army Natick Laboratories Natick, Massachusetts 01760

13. ABSTRACT

In order to develop techniques for studying the transient behavior of plastic materials subjected to mechanical impact, a preliminary photographic investigation was undertaken with an electronic image converter camera system. Two types of events were recorded with CR-39 plastic serving as the specimen material:

1. Stress pulses, produced in the plastic by mechanical impaction, were studied by observation of the resulting fringe patterns. The pulse fronts were characterized in terms of shape and propagation velocity. An empirical equation was derived to express the decrease in slope of segments of the pulse front as it propagated through the specimen.

2. Propagating cracks, generated in the plastic by mechanical impact, were subjected to photographic analysis. Crack propagation velocities and estimated crack initiation times were obtained. These served to yield a rough estimate of the magnitude of the incident longitudinal pulse level at which crack initiation occurred.

DD FORM 1 JAN 64 1473

Unclassified
Security Classification

14. KEY WORDS	LINK A		LINK B		LINK C	
	ROLE	WT	ROLE	WT	ROLE	WT
Measurement	8		8			
Wave propagation	9					
Stresses	9					
Impact	9		9			
Crack propagation			9			
Velocity			9			
Plastics	9		9			
Transparent	0		0			
High speed photography	10		10			

INSTRUCTIONS

1. ORIGINATING ACTIVITY: Enter the name and address of the contractor, subcontractor, grantee, Department of Defense activity or other organization *(corporate author)* issuing the report.

2a. REPORT SECURITY CLASSIFICATION: Enter the overall security classification of the report. Indicate whether "Restricted Data" is included. Marking is to be in accordance with appropriate security regulations.

2b. GROUP: Automatic downgrading is specified in DoD Directive 5200.10 and Armed Forces Industrial Manual. Enter the group number. Also, when applicable, show that optional markings have been used for Group 3 and Group 4 as authorized.

3. REPORT TITLE: Enter the complete report title in all capital letters. Titles in all cases should be unclassified. If a meaningful title cannot be selected without classification, show title classification in all capitals in parenthesis immediately following the title.

4. DESCRIPTIVE NOTES: If appropriate, enter the type of report, e.g., interim, progress, summary, annual, or final. Give the inclusive dates when a specific reporting period is covered.

5. AUTHOR(S): Enter the name(s) of author(s) as shown on or in the report. Enter last name, first name, middle initial. If military, show rank and branch of service. The name of the principal author is an absolute minimum requirement.

6. REPORT DATE: Enter the date of the report as day, month, year; or month, year. If more than one date appears on the report, use date of publication.

7a. TOTAL NUMBER OF PAGES: The total page count should follow normal pagination procedures, i.e., enter the number of pages containing information.

7b. NUMBER OF REFERENCES: Enter the total number of references cited in the report.

8a. CONTRACT OR GRANT NUMBER: If appropriate, enter the applicable number of the contract or grant under which the report was written.

8b, 8c, & 8d. PROJECT NUMBER: Enter the appropriate military department identification, such as project number, subproject number, system numbers, task number, etc.

9a. ORIGINATOR'S REPORT NUMBER(S): Enter the official report number by which the document will be identified and controlled by the originating activity. This number must be unique to this report.

9b. OTHER REPORT NUMBER(S): If the report has been assigned any other report numbers *(either by the originator or by the sponsor)*, also enter this number(s).

10. AVAILABILITY/LIMITATION NOTICES: Enter any limitations on further dissemination of the report, other than those imposed by security classification, using standard statements such as:

(1) "Qualified requesters may obtain copies of this report from DDC."

(2) "Foreign announcement and dissemination of this report by DDC is not authorized."

(3) "U. S. Government agencies may obtain copies of this report directly from DDC. Other qualified DDC users shall request through _____."

(4) "U. S. military agencies may obtain copies of this report directly from DDC. Other qualified users shall request through _____."

(5) "All distribution of this report is controlled. Qualified DDC users shall request through _____."

If the report has been furnished to the Office of Technical Services, Department of Commerce, for sale to the public, indicate this fact and enter the price, if known.

11. SUPPLEMENTARY NOTES: Use for additional explanatory notes.

12. SPONSORING MILITARY ACTIVITY: Enter the name of the departmental project office or laboratory sponsoring *(paying for)* the research and development. Include address.

13. ABSTRACT: Enter an abstract giving a brief and factual summary of the document indicative of the report, even though it may also appear elsewhere in the body of the technical report. If additional space is required, a continuation sheet shall be attached.

It is highly desirable that the abstract of classified reports be unclassified. Each paragraph of the abstract shall end with an indication of the military security classification of the information in the paragraph, represented as *(TS), (S), (C), or (U).*

There is no limitation on the length of the abstract. However, the suggested length is from 150 to 225 words.

14. KEY WORDS: Key words are technically meaningful terms or short phrases that characterize a report and may be used as index entries for cataloging the report. Key words must be selected so that no security classification is required. Identifiers, such as equipment model designation, trade name, military project code name, geographic location, may be used as key words but will be followed by an indication of technical context. The assignment of links, rules, and weights is optional.